Multi-Channel Longitudinal Power Profile Estimation

Inwoong Kim[(1)], Olga Vassilieva[(1)], Ryu Shinzaki[(2)], Motohiko Eto[(2)], Shoichiro Oda[(2)], Paparao Palacharla[(1)]

[(1)] Fujitsu Network Communications, Inc., 2801 Telecom Parkway, Richardson, TX 75082, USA
[(2)] Fujitsu Limited, 1-1 Kamikodanaka 4-Chome, Nakahara-ku, Kawasaki, Kanagawa 211-8588, Japan
inwoong.kim@fujitsu.com

Abstract *We propose multi-channel power profile estimation considering both XPM and SPM. We achieve improved estimation accuracy by applying multi-bandpass filter and can effectively alleviate the impact of misalignment of waveforms combined in MC-PPE by minimizing the mean-square-error through off-line processing in digital domain. ©2023 The Author(s)*

Introduction

Longitudinal power profile estimation (PPE) based on coherent receiver provides end-to-end transmission link monitoring such as anomaly localization [1,2]. The advantage of PPE, enabling multi-span monitoring without any additional hardware, has motivated increasing research that includes correlation-based PPE, NN-DBP (neural network – digital back propagation)-based PPE, VNEQ (Volterra nonlinear equalizer)-based PPE, and linear least-square method, where reference waveform and emulated waveforms are evaluated to find longitudinal power profiles [1-6]. Coherent receiver-based PPE is possible due to noncommutative properties of dispersion and nonlinear operators. Recently, impressive measurement of power profile and anomaly detection in submarine transmission link of about 10000 km is demonstrated [7]. Interestingly, there was another approach to characterizing longitudinal power profile by evaluating XPM between channels based on pulse collision model in contrast to coherent receiver-based PPEs utilizing SPM in a channel [8]. [9] showed that XPM may degrade the performance of PPE especially where optical power becomes small in transmission links.

In this paper, we propose multi-channel PPE (MC-PPE) that utilizes both SPM and XPM effects in multi-channel configurations achieving improved accuracy of PPE especially where optical power is low towards the end of transmission link due to fiber attenuation. We describe the MC-PPE technique and demonstrate significantly improved performance compared to SC (single-channel)-PPE. We also address the impact of waveform misalignments between channels that may occur when waveforms from multiple channels are combined for MC-PPE. Furthermore, we describe how these misalignments can be easily corrected in the digital domain via off-line process.

Multi-Channel PPE

MC-PPE can exploit XPM effect between channels to improve the estimation accuracy compared to SC-PPE. Similar to multi-channel digital backpropagation (MC-DBP), where split-step Fourier method (SSFM) is applied to the combined electric field of all channels, MC-PPE is applied to combined waveforms to include SPM and XPM effects [10-11].

Schematic diagram of multi-channel transmission and architecture for MC-PPE is shown in Fig. 1. We assume transmitted signals travel along common optical transmission links. In general, coherent receiver-based PPE requires waveform at the transmitter side and reference waveform at the receiver side. The waveform at the transmitter side can be rebuilt based on the demodulated symbols or recovered data at the receiver side [1-6]. For MC-PPE, waveforms from multiple channels should be combined into an aggregate waveform. This can be achieved by adding two waveforms after upsampling (using zero-padding) of single channel waveforms and appropriate frequency shift as shown in Fig. 1. The upsampling bandwidth should be larger than the aggregate bandwidth of channels including the channel

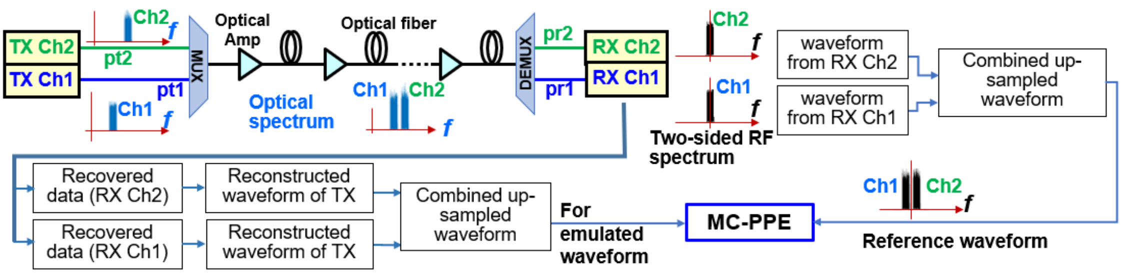

Fig. 1: Schematic diagram of transmission system and architecture for MC-PPE.

spacing. Let's say $A_1(t_n)$ and $A_2(t_n)$ are up-sampled waveforms of the first and second channels respectively, where t_n is discrete resampling time. Then, the combined waveform can be calculated by $A_c(t_n) = A_1(t_n)*exp(-i\pi\Delta_{Ch}t_n) + A_2(t_n)*exp(i\pi\Delta_{Ch}t_n)$ where Δ_{Ch} is channel spacing and the 2nd channel is assumed to have higher optical carrier frequency.

In general, coherent receiver does not oversample, that means the combined waveform for reference (receiver side) does not have any nonlinear interference (NLI) noise outside of each channel bandwidth. But transmitted waveform by emulation does have NLI noise outside of each channel that causes performance degradation in MC-PPE where power profile is found by optimizing transmission emulation parameters over links with multiple segments to minimize MSE (mean square error) between reference and emulated waveforms. Thus, multi-bandpass filter (MBPF) is applied in emulation to suppress NLI noise outside of each channel. For this, we need to modify the first order nonlinear perturbation term for the k-th segment of optical link, eq. (1) in [6], by applying MBPF operator $\hat{F}$ as

$$j\gamma'_k \Delta z_k \left\{ \hat{F}\hat{H}(L - z_k)\left[\hat{N}\left(\hat{H}(z_k)A(0,m) \right) \right] \right\} \quad (1)$$

where γ'_k is product of power at k-th segment and nonlinear coefficient, $\hat{H}$ is linear operator for dispersion, $\hat{N}$ is nonlinear operator, Δz_k is step size at z_k, L is transmission distance, and A is input waveform. Frequency response of the filter has 1 for 1.1*baudrate of each channel and 0 otherwise.

In addition, there may be misalignment errors between two waveforms when they are combined in digital domain for MC-PPE. First, there could be an error in channel spacing since independent laser frequencies for optical carriers may drift by environmental perturbation. Second, there may be an error in time frames to be combined because non-common optical path between transponders and optical multiplexer or demultiplexer (e.g., pt1 and pt2 or pr1 and pr2 in Fig. 1) may cause relative time delay even though clocks for transponders are shared. Third, there may be misalignment of SOPs because of random rotation of polarization in non-common optical path by environmental perturbation. Thus, X-pol signal of the first channel may not be aligned to the X-pol of the second channel at optical multiplexer. We evaluate the impact of misalignment between channels for MC-PPE and show that it can be easily corrected in the digital domain via off-line processing.

System Modeling for PPE

We transmit 2 or 3 channels with Nyquist pulse shaped 96-Gbaud DP-16QAM signals over 5 spans x 80 km SSMF fiber (dispersion coefficient 17e-6 s/m^2, dispersion slope 57 s/m^3, and

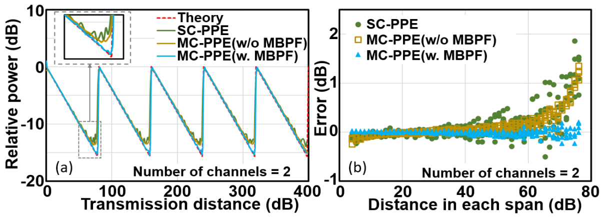

Fig. 2: (a) Power profiles depending on PPEs (inset range: 50 km – 85 km), (b) Estimation error in each span.

nonlinear coefficient 1.3 /W/km). Channel spacing is 125 GHz. 10 different patterns of 2^{15} symbols are transmitted for evaluation. For high accuracy, 32 samples per symbols, that is much larger than WDM channel bandwidth, and fine step size of 0.1 km are used to solve Manakov equation with SSFM. Launch power is 4.8 dBm per channel. Ideal optical amplifier is used to compensate optical loss, where noise figure is set to zero to observe the impact from XPM in PPE. Transmitter and receiver side waveforms are saved for each channel with 2 samples per symbol after filtering for Nyquist channel. For SC-PPE, PPE based on minimum MSE with complex scaling factor is carried out for one channel [6]. For MC-PPE, PPE is carried out over combined channels after upsampling to emulate WDM bandwidth. Emulation step size is adjusted accordingly to the WDM channel bandwidth. In both cases, the results are averaged over 10 different data patterns to improve the accuracy. For comparison, RMSE (root-MSE) and maximum error from theoretical estimation are calculated from 3 km to 77 km of each span, where regions around vertical transition of power by amplifier are excluded.

Performance Evaluation

Fig. 2 (a) shows the estimated power profile with SC-PPE (60 steps/span) and MC-PPE (60 steps/span after resampling of 240 steps/span for transmission emulation) in 2-channel transmission. SC-PPE and MC-PPE without MBPF showed lower accuracy than MC-PPE with MBPF, as shown in inset, in the area of small optical power in optical links. MC-PPE with MBPF shows almost matched profile with the theoretical estimation even in low signal power area. The estimation errors for various PPE techniques are shown in Fig. 2 (b). The estimation error is plotted with respect to distance from the beginning of each span. The error tends to increase as distance increases due to reduced NLI noise by fiber attenuation. MC-PPE with MBPF improves the PPE performance while the performance is limited without MBPF. The RMSE and maximum error are 0.37 dB and 1.86 dB for SC-PPE, 0.27 dB and 1.35 dB for MC-PPE without MBPF, and 0.054 dB and 0.25 dB for MC-PPE with MBPF. Fig. 3 (a) shows the estimated power profile depending on PPE when 3 channels (60

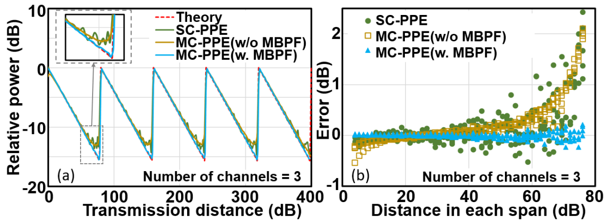

Fig. 3: (a) Power profiles depending on PPEs (inset range: 50 km – 85 km), (b) Estimation error in each span.

steps/span after resampling of 300 steps/span for transmission emulation) are transmitted. Similar trend is observed as in Fig. 2. MC-PPE with MBPF shows the best performance close to the theoretical estimation and the smallest distribution of errors as shown in Fig. 3 (b). The RMSE and maximum error are 0.47 dB and 2.43 dB for SC-PPE, 0.46 dB and 2.1 dB for MC-PPE without MBPF, and 0.052 dB and 0.22 dB for MC-PPE with MBPF. SC-PPE shows worse results with 3-channel transmission compared to 2-channel transmission due to increased XPM while MC-PPE with MBPF shows slightly lower error with 3-channel transmission. These results demonstrate that MC-PPE can improve accuracy with larger number of WDM channels in contrast to SC-PPE. And it is important to apply MBPF in emulation for MC-PPE to suppress NLI noise outside of each channel spectrum to improve accuracy.

Impact of misaligned waveforms in MC-PPE

We analyse the impact of misalignment of waveforms between channels when they are combined into a waveform in MC-PPE. We evaluate minimum MSE between emulated and reference of combined waveforms of two channels along with the power profile estimated by MC-PPE. In this study, only a data pattern with

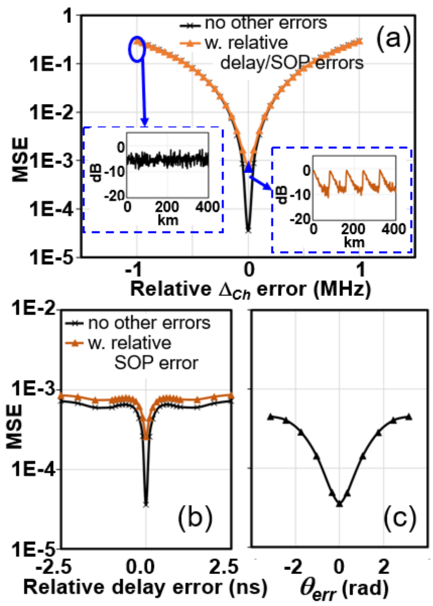

Fig. 4: MSE with (a) channel spacing error, (b) relative delay error, (c) relative SOP error.

2^{15} symbols is used. We found that the impact of relative phase error (or relative rotation of constellation) between two channels is negligible. The maximum variation of MSE depending on relative phase error is about only 10% and estimated power profile is almost identical without regards to this error. Thus, we ignore possible relative phase errors between channels. Fig. 4 (a) shows the MSE depending on channel spacing error. The black line shows the case without other errors and the orange line is with other errors; relative delay error of 4 ns and relative SOP error (rotating SOP of the second channel with azimuthal angle of 1 rad and ellipticity angle of 1 rad). The inset figure with black line shows that MC-PPE fails when there is large channel spacing error (e.g., 1MHz) while the other inset figure shows estimated power profile proportional to actual power profile even with other errors when the MSE is minimized. That means, channel spacing error can be minimized by minimizing MSE. Note that MC-PPE still can show some power profile (inset with orange line) even though there is large error in relative time delay and relative SOP between channels.

Fig. 4 (b) shows MSE depending on relative delay error between waveforms of two channels to be combined. The minimum MSE occurs when relative delay error is zero without regards to SOP misalignment. Thus, MSE can be used to minimize relative delay between waveforms of channels.

Fig. 4 (c) shows MSE depending on the relative azimuthal errors (θ_{err}) of SOP of two channels. The impact is not significant as the other two errors and the minimum MSE corresponds to where θ_{err} become zeros. Based on this study we conclude that the misalignment of waveforms of multi-channels can be minimized by minimizing MSE. First, channel spacing can be corrected, then relative delay error can be corrected, and lastly, the relative SOP error can be minimized for optimal operation of MC-PPE. For MC-PPE with 3 channels, first 2 channels can be aligned, then the third channel can be aligned.

Conclusion

We proposed multi-channel-PPE to improve accuracy of PPE by considering the XPM impact and demonstrated superior performance with multi-BPF, even when optical power is low at the end of transmission link. We also evaluated the impact of misalignment of waveforms in MC-PPE and showed that optimal alignment between channels can be realized by minimizing MSE through off-line processing in digital domain. This improved accuracy of MC-PPE can simplify operations and troubleshooting of disaggregated optical networks.

References

[1] T. Tanimura, K. Tajima, S. Yoshida, S. Oda, and T. Hoshida, “Experimental Demonstration of a Coherent Receiver that Visualizes Longitudinal Signal Power Profile over Multiple Spans out of Its Incoming Signal,” *presented at European Conference on Optical Communication (ECOC)*, Dublin, Ireland, 2019. DOI: 10.1049/cp.2019.1031

[2] T. Sasai, M. Nakamura, E. Yamazaki, S. Yamamoto, H. Nishizawa, and Y. Kisaka, “Digital Longitudinal Monitoring of Optical Fiber Communication Link,” *Journal of Lightwave Technology*, vol. 40, no. 8, pp. 2390-2408, 2022. DOI: 10.1109/JLT.2021.3139167

[3] T. Sasai, M. Nakamura, T. Kobayashi, H. Kawakami, E. Yamazaki, and Y. Kisaka, "Revealing Raman-amplified Power Profile and Raman Gain Spectra with Digital Backpropagation," *presented at Optical Fiber Communications Conference and Exhibition (OFC)*, San Francisco, USA, 2021. DOI: 10.1364/OFC.2021.M3I.5

[4] S. Gleb, P. Konstantin, J. Luo, and B. Zheng, “Fiber link anomaly detection and estimation based on signal nonlinearity,” *presented at European Conference on Optical Communication (ECOC)*, Bordeaux, France, 2021. DOI: 10.1109/ECOC52684.2021.9606094

[5] T. Sasai, E. Yamazaki, M. Nakamura, and Y. Kisaka, “Proposal of Linear Least Squares for Fiber-Nonlinearity-Based Longitudinal Power Monitoring in Multi-Span Link,” *presented at OptoElectronics and Communications Conference (OECC)*, Toyama, Japan, 2022. DOI: 10.23919/OECC/PSC53152.2022.9850175

[6] I. Kim, O. Vassilieva, R. Shinzaki, M. Eto, S. Oda, and P. Palacharla, “Robust Longitudinal Power Profile Estimation in Optical Networks using MMSE with Complex Scaling Factor,” *presented at Optical Fiber Communications Conference and Exhibition (OFC)*, San Diego, USA, W4H.6, 2023.

[7] A. May, F. Boitier, A. Carbo Meseguer, J. U. Esparza, P. Plantady, A. Calsat, and P. Layec, “Longitudinal Power Monitoring Over a Deployed 10,000-km Link for Submarine Systems,” *presented at Optical Fiber Communications Conference and Exhibition (OFC)*, San Diego, USA, Tu2G.3, 2023.

[8] P. Serena, C. Lasagni, A. Bononi, F. Boitier, A. May, P. Ramantanis, M. Lonard, "Locating Fiber Loss Anomalies with a Receiver-Side Monitoring Algorithm Exploiting Cross-Phase Modulation," *presented at Optical Fiber Communications Conference and Exhibition (OFC)*, San Diego, USA, W1H.3, 2023.

[9] I. Kim, O. Vassilieva, R. Shinzaki, M. Eto, S. Oda, and P. Palacharla, “Longitudinal Power Profile Estimation in WDM Transmission and Optical Network Tomography (invited),” *is submitted to OptoElectronics and Communications Conference (OECC)*, Shanghai, China, 2023.

[10] X. Li, X. Chen, G. Goldfarb, E. Mateo, I. Kim, F. Yaman, and G. Li, “Electronic post-compensation of WDM transmission impairments using coherent detection and digital signal processing,” *Optics Express*, vol. 16, no. 2, pp. 880-888, 2008. DO I: 10.1364/OE.16.000880

[11] G. Liga, T. Xu, A. Alvarado, R. I. Killey, and P. Bayvel, “Electronic post-compensation of WDM transmission impairments using coherent detection and digital signal processing,” *Optics Express*, vol. 22, no. 24, pp. 30053-30062, 2014. DOI: 10.1364/OE.22.030053